PHARMACOKINETICS, PHARMACODYNAMICS AND DRUG METABOLISM

The Transient Dermal Exposure: Theory and Experimental Examples Using Skin and Silicone Membranes

H. FREDERICK FRASCH, ANA M. BARBERO

Health Effects Laboratory, National Institute for Occupational Safety and Health, Morgantown, West Virginia 26505

Received 20 December 2006; revised 15 March 2007; accepted 7 April 2007

Published online in Wiley InterScience (www.interscience.wiley.com). DOI 10.1002/jps.21035

ABSTRACT: A diffusion model is presented to account for the disposition of chemicals applied to skin as transient exposures. Two conditions are considered that apply to the skin surface following the exposure period, which are applicable to chemicals exhibiting two extremes of chemical volatility. For one case, representing highly volatile compounds, the solution is generalized to apply to multiple transient exposures. For both cases, algebraic expressions are derived to calculate the total amount of chemical that penetrates the skin. The theory is applied to experimental measurements of the *in vitro* penetration of diethyl phthalate applied to hairless guinea pig (HGP) skin and silicone rubber membranes (SRMs) as transient exposures. The transient exposure theory ably models the experimental data, with coefficients of determination greater than 0.97 (HGP) and greater than 0.99 (SRM). The ability of parameters derived from concurrent infinite dose experiments to predict the time course of absorption from transient exposures is explored. Discrepancies were found between measured cumulative penetration of chemical from transient exposure experiments and penetration predicted from parameters derived from infinite dose experiments, particularly for HGP. Possible reasons are explored. The current model may provide a realistic framework for estimating absorption from occupational, environmental and pharmaceutical dermal exposures. J Pharm Sci 97:1578–1592, 2008

Keywords: skin; permeability; diffusion; transdermal; mathematical model; membrane transport; passive diffusion/transport; percutaneous; transdermal drug delivery

INTRODUCTION

Many exposures of chemicals to skin do not reach a steady state rate of absorption. In industrial and environmental exposures, individuals may be transiently exposed following dermal contact until the chemical is washed off or evaporates. In cosmetic applications, exposures to perfume or fragrance materials and vehicles may be short lived, and in pharmaceutical applications, non steady state conditions are important considerations in, for example, absorption from dermal patches.

In contrast to these realistic exposures, most skin permeation studies have been performed

Correspondence to: H. Frederick Frasch (Telephone: 304-285-5755; Fax: 304-285-6041; E-mail: hbf9@cdc.gov)

Journal of Pharmaceutical Sciences, Vol. 97, 1578–1592 (2008)

by measuring the steady state rate of dermal absorption from large doses. From these measurements the skin permeability coefficient (k_p) is derived, which is the skin's conductance to a chemical from a particular vehicle. The amount of chemical penetrating the skin can be estimated from these measurements, but the calculation is valid only for the steady state and does not take into consideration the transient absorption that occurs during the initial stages of exposure, nor does it include absorption that persists after removal of the chemical. Transient conditions need to be considered for a full and accurate accounting of dermal disposition from skin exposures.

Some previous studies have not employed large doses but instead have examined the finite dose regime,[1–7] where a small amount of chemical is applied to the skin and its disposition is followed as the dose depletes from the skin surface through absorption and possibly evaporation. In the present study, we investigate a related but different exposure scenario. In the transient exposure considered here, a donor chemical is applied to the skin and removed at a later time, possibly prior to establishment of steady state and before significant depletion of the chemical has occurred. This scenario differs from the finite dose exposure in that total absorption depends, among other variables, on the time of exposure of the skin to the chemical. Both exposure regimes are relevant to "real world" exposures. The transient exposure scenario might occur in the workplace, for example, when a worker splashes some chemical on his skin and effectively washes it some time later. A full accounting of the disposition of applied chemical in such an exposure requires consideration of the fate of chemical that resides in the skin after the chemical is removed.

In these studies, theory is first developed to solve for the diffusion of chemical from transient exposures. Analytical solutions, applicable to an effective homogeneous membrane, are obtained in the Laplace domain for concentration and flux distributions and mass accumulation at the lower membrane surface. Two cases are presented that represent two extremes of volatility of the applied chemical, and for one case the solution is generalized for multiple transient exposures. The theory predicts that parameters that can be derived from infinite dose permeation experiments (permeability and lag time), should enable the prediction of the time course of mass accumulation for the transient exposures. Diffusion cell experiments are described that explore the validity of the developed theory. Numerical inversion of the Laplace domain solutions permits comparison of the theoretical models with experimental results. Skin from hairless guinea pigs was used, and silicone rubber membranes (SRMs) were also studied to examine the legitimacy of the homogeneous membrane approximation. By manipulating the post exposure boundary conditions, we were able to mimic the effects of both extremes of chemical volatility with one model compound. Infinite dose experiments were run concurrently with the transient exposure experiments, permitting a comparison among all three exposures of derived penetration parameters permeability and lag time.

To our knowledge these Laplace domain solutions have not hitherto been published, although time domain solutions can be arrived at using well-known solutions for the time during which the skin is exposed to chemical,[8] combined with heat conduction solutions presented by Carslaw and Jaeger[9] that can be adapted for use following the exposure period. The latter are complicated and not directly usable in their published form. The solutions require evaluation of an infinite number of terms of a non trivial definite integral, where each term itself contains an infinite number of terms, and also require the solution of a transcendental equation for each term. Of course, for practical purposes the series can be truncated to a manageable number of terms, but for small values of time a larger number of terms are required. The overall simpler approach of numerical inversion of the Laplace solutions, and the ability to solve the equations for both large and small values of time to within a defined error, make this approach superior in our estimation.

THEORETICAL FRAMEWORK

The skin is modeled as an effective homogeneous membrane (Fig. 1). This means that the macro diffusion properties of a heterogeneous structure such as skin can be described in terms of effective transport properties for an equivalent homogeneous membrane.[10–12] Different exposure conditions are considered, but for all cases the membrane is initially free of chemical and at the lower surface ($x = h$), zero concentration (sink condition) is maintained for all time. At the upper surface ($x = 0$) the skin is exposed to a chemical of concentration C_1 for a finite time T_1, after which

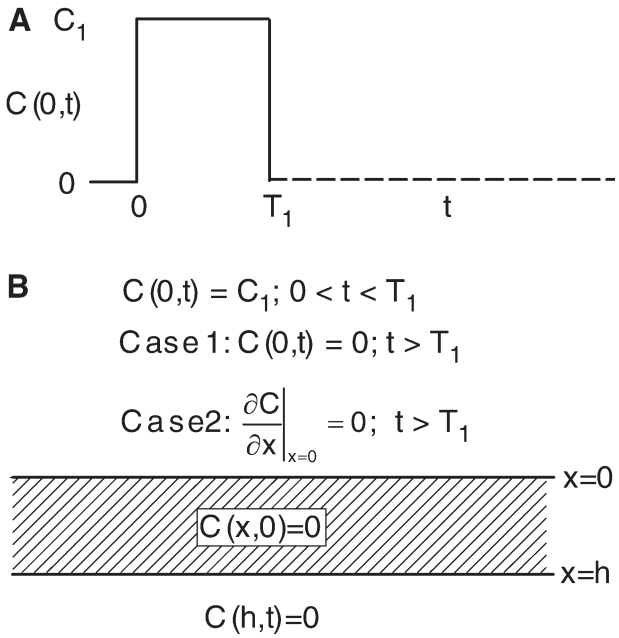

Figure 1. Schematic of effective homogeneous membrane diffusion model. A: Input concentration of transient exposure. A chemical of concentration C_1 is applied to the surface of the membrane at time $t=0$ and removed at time $t=T_1$. Dashed line following T_1 indicates that boundary concentration is not necessarily defined for that time. B: Initial and boundary conditions for transient exposure model. The membrane is initially free of permeant ($C(x, 0)=0$), and sink conditions exist at the lower boundary for all time ($C(h, t)=0$). For Case 1, surface concentration is specified following the exposure time (sink condition; $C(0, t)=0$ for $t > T_1$). For Case 2, flux is specified after the exposure (zero flux; $\partial C/\partial x|_{x=0} = 0$ for $t > T_1$).

the chemical is completely removed. Two boundary conditions are considered for the time following the exposure. These represent conditions that apply to exposures to chemicals that exhibit two extremes of volatility. In Case 1, zero concentration is imposed on the skin surface for time greater than T_1. This sink condition applies to highly volatile chemicals that evaporate rapidly from the skin surface and dissipate in ambient air. It also represents the case where the chemical is removed from the skin from a continuous rinse or solvent immersion for a time much longer than the lag time of the membrane. In Case 2, zero flux is imposed on the skin surface for time greater than T_1. This boundary condition applies to nonvolatile chemicals that partition preferentially in skin as opposed to the surrounding air. Intermediate volatilities require specification of the volatile flux at the skin surface and will be considered in a subsequent study.

Analytical solutions for concentration and flux distributions and mass accumulation at the membrane surfaces are obtained in the Laplace domain. For Case 1, the solution is generalized for multiple or repeated transient dermal exposures of varying concentrations and durations. For all transient dose cases, the total amounts of chemical that penetrate the skin are given by algebraic equations. For Case 1, the equation is quite simple and does not depend on membrane lag time.

We seek solutions for concentration C of the one-dimensional diffusion equation:

$$\frac{\partial C}{\partial t} = D\frac{\partial^2 C}{\partial x^2} \tag{1}$$

where D is (constant) effective diffusivity, t is time and x is position. The flux or rate at which the diffusing substance emerges from unit area is given by:

$$f(x, t) = -D\frac{\partial C}{\partial x} \tag{2}$$

This expression evaluated at the lower surface $x=h$, then integrated with respect to t, gives the total mass accumulation per unit area that has passed through the membrane in time t:

$$m(t) = \int_0^t f(h, t)\mathrm{d}t \tag{3}$$

In diffusion cell experiments, this is the total mass accumulation measured in receptor fluid.

Transient Dose Exposure Conditions

A chemical of concentration C_1 is applied at time $t=0$ to the upper surface of a membrane and removed at $t=T_1$. Two boundary conditions after the exposure time are explored here.

Case 1: Zero Concentration (Sink Condition) at Upper Surface

After the initial exposure, the concentration at the surface of the skin is maintained at zero. This boundary condition corresponds to an infinite, well-stirred reservoir on the skin surface and represents the idealized case of a highly volatile compound. As chemical diffuses upward to the skin surface from deeper skin regions, it immediately evaporates from the surface and diffuses freely into surrounding air and is carried

 DOI 10.1002/jps

away by ambient air currents. For this condition, the Laplace domain solution of Eq. (1) is:

$$\hat{C}(x) = \frac{K_{mv}C_1(1-e^{-sT_1})\sinh[\lambda(h-x)]}{s\sinh(\lambda h)} \quad (4)$$

A circumflex indicates a Laplace domain function of the complex variable s, and $\lambda = \sqrt{s/D}$. K_{mv} is the membrane-vehicle partition coefficient. Flux is given by:

$$\hat{F}(x) = -D\frac{d\hat{C}}{dx} = \frac{K_{mv}C_1D\lambda(1-e^{-sT_1})\cosh[\lambda(h-x)]}{s\sinh(\lambda h)} \quad (5)$$

and the mass accumulation per unit area below the skin is:

$$\hat{M} = \frac{\hat{F}(h)}{s} = \frac{K_{mv}C_1D\lambda(1-e^{-sT_1})}{s^2\sinh(\lambda h)} \quad (6)$$

The total mass accumulation, that is mass accumulation as time approaches infinity, can be determined from the Final Value Theorem of Laplace transform theory:

$$m_\infty = A\lim_{t\to\infty} m(t) = A\lim_{s\to 0} s\hat{M} = AK_{mv}\frac{D}{h}C_1T_1 = k_pAC_1T_1 \quad (7)$$

where A is the area of skin exposed to chemical and $k_p = K_{mv}\,D/h$ is the permeability coefficient, with K_{mv} the membrane-vehicle partition coefficient.

For the general case of multiple (n) intermittent exposures of concentrations C_i and durations T_i, delayed by times T_{di}, the applied surface concentration can be represented as

$$C_s = C(0,t) = \sum_{i=1}^{n} C_i[u(t-T_{di}) - u(t-(T_{di}+T_i))] \quad (8)$$

where

$$u(t-\Delta) = \begin{bmatrix} 1 & t>\Delta \\ 0 & t<\Delta \end{bmatrix}$$

is defined as the shifted unit step function. (In the limiting case of $n=1$, this reduces to the single transient exposure considered above if $T_{d1}=0$.) For this multiple exposure, the concentration, flux and mass accumulation are:

$$\hat{C}(x) = \frac{\sinh[\lambda(h-x)]}{s\sinh(\lambda h)}K_{mv}\sum_{i=1}^{n} C_ie^{-sT_{d_i}}(1-e^{-sT_i}) \quad (9)$$

$$\hat{F}(x) = \frac{D\lambda\cosh[\lambda(h-x)]}{s\sinh(\lambda h)}K_{mv}\sum_{i=1}^{n} C_ie^{-sT_{d_i}}(1-e^{-sT_i}) \quad (10)$$

$$\hat{M} = \frac{D\lambda}{s^2\sinh(\lambda h)}K_{mv}\sum_{i=1}^{n} C_ie^{-sT_{d_i}}(1-e^{-sT_i}) \quad (11)$$

The total mass accumulation is:

$$m_\infty = k_p\sum_{i=1}^{n} A_iC_iT_i \quad (12)$$

Case 2: Zero Flux at Upper Surface

After the exposure period, the upper skin surface presents an impermeable barrier to diffusion. This represents the case of a non volatile compound, for which the skin is the preferred environment for the chemical as opposed to the surrounding air. The solutions for $t \le T_1$ are the same as for Case 1. For $t > T_1$:

$$\hat{C}(x) = \frac{R_0\sinh(\lambda[h-x]) - R_h\lambda\cosh(\lambda x)}{\lambda\cosh(\lambda h)} + C_p(x) \quad (13)$$

where

$$R_0 = -\frac{C_1}{sh} - \frac{2C_1}{\pi}\sum_{n=1}^{\infty}\frac{k_n}{n(Dk_n^2+s)}\exp(-DT_1k_n^2) \quad (14)$$

$$R_h = -\frac{2C_1}{\pi}\sum_{n=1}^{\infty}\frac{\sin(k_nh)}{n(Dk_n^2+s)}\exp(-DT_1k_n^2) \quad (15)$$

$$C_p(x) = \frac{C_1}{s} - \frac{C_1x}{sh} - \frac{2C_1}{\pi}\sum_{n=1}^{\infty}\frac{\sin(k_nx)}{n(Dk_n^2+s)}\exp(-DT_1k_n^2) \quad (16)$$

with $k_n = n\pi/h$.

Flux is given by

$$\hat{F}(x) = -D\frac{d\hat{C}}{dx} = D\left(\frac{R_0\lambda\cosh(\lambda[h-x]) + R_h\lambda^2\sinh(\lambda x)}{\lambda\cosh(\lambda h)}\right) - D\frac{dC_p}{dx} \quad (17)$$

where

$$\frac{dC_p}{dx} = -\frac{C_1}{sh} - \frac{2C_1}{\pi}\sum_{n=1}^{\infty}\frac{k_n\cos(k_n x)}{n(Dk_n^2+s)}\exp(-DT_1k_n^2) \quad (18)$$

Additional ($t > T_1$) mass accumulation is given by:

$$\hat{M} = \frac{\hat{F}(h)}{s} \quad (19)$$

The total mass accumulation as time approaches infinity is most easily calculated as the sum of the amount in the membrane at time $t = T_1$:

$$m_m = \frac{AhC_1}{2}\left[1 - \frac{8}{\pi^2}\sum_{n=0}^{\infty}\frac{1}{(2n+1)^2}\exp(-D(2n+1)^2\pi^2T_1/h^2)\right] \quad (20)$$

plus the amount that has passed through the membrane at time $t = T_1$:

$$m_{T_1} = AhC_1\left[\frac{DT_1}{h^2} - \frac{1}{6} - \frac{2}{\pi^2}\sum_{n=1}^{\infty}\frac{(-1)^n}{n^2}\exp(-Dn^2\pi^2T_1/h^2)\right] \quad (21)$$

Both quantities are given by Crank.[8] The sum, rewritten in terms of permeability coefficient and lag time, yields:

$$m_\infty = k_pAC_1\left[T_1 + 2\tau - \frac{12\tau}{\pi^2}\sum_{n=1}^{\infty}\frac{1}{n^2}\exp\left(-\frac{n^2\pi^2T_1}{6\tau}\right)\right] \quad (22)$$

Where $\tau = h^2/(6D)$ is the membrane lag time.

For relatively long exposure times compared to lag time, the terms in the exponential series become insignificant. For example, for $T_1 \geq \tau$, the error is <10% if the infinite series is ignored. In this case, Eq. (22) can be approximated as:

$$m_\infty \approx k_pAC_1(T_1 + 2\tau) \quad (23)$$

For very long exposure times ($T_1 \gg 2\tau$), it follows that

$$m_\infty \approx k_pAC_1T_1 \quad (24)$$

which is the same as Eq. (7). That is, at this limit the total mass accumulation in Case 2 is similar to that in Case 1. An equivalent condition exists when lag time is very small. As $\tau \to 0$, total mass accumulation in Case 2 is also similar to that in Case 1 and is given by Eq. (24).

Time Domain Solutions

Time domain solutions of the Laplace domain equations for concentration and flux distribution and mass accumulation over time are obtained by numerical inversion using Scientist (MicroMath Scientific Software, Salt Lake City, UT). This software implements both Weeks' and Piessens' methods of numerical inversion.

EXPERIMENTAL METHODS

In vitro diffusion cell experiments were undertaken to investigate the applicability of the transient exposure theory outlined above. Diethyl phthalate (DEP) was used as a low volatility model compound (CAS: 84-66-2; $MW = 222.2$; log $K_{ow} = 2.47$; vapor pressure $= 2.1 \times 10^{-3}$ mmHg at 25°C).[13] DEP is widely used as a stabilizing agent in perfumes and other cosmetic formulations.[14]

For these experiments, both hairless guinea pig skin and homogeneous SRMs were used. Side-by-side diffusion cells allowed us to approximate both of the idealized post exposure boundary conditions (Cases 1 and 2), in addition to the infinite dose condition, using one compound.

Hairless Guinea Pig Skin Experiments

Male hairless guinea pigs (HGPs), ~500 g, of the strain Crl:IAF(HA)-hrBR were obtained from Charles River Laboratories (Wilmington, MA)

 DOI 10.1002/jps

and their use was approved by our Animal Care and Use Committee. HGPs were euthanized with CO_2 and back skin was harvested and used the same day. Skin was dermatomed (Padgett Model B, Integra LifeSciences, Plainsboro, NJ) at a setting of 315 μm thickness. Skin discs were obtained using a $^3/_4''$ circular stainless steel punch, weighed and mounted onto diffusion cells. A blocked experimental design was implemented in which each HGP contributed skin discs to each of three experimental protocols.

From each of 8 HGPs, 6 skin punches were mounted on horizontal (side-by-side) diffusion cells (Perme-Gear, Bethlehem, PA) and the receptor compartments were filled with warmed, degassed buffer. Buffer consisted of HEPES-buffered Hank's balanced salt solution. 5.96 g HEPES free acid was stirred into 1000 mL of Hank's. Then 0.32 g of $NaHCO_3$ and 0.05 g gentamycin sulfate were added. The pH was brought to 7.40 at 37°C by drop wise addition of 6N NaOH.

Receptor and donor volumes were 5 ml and the diameter of exposed skin was 9 mm. Receptor and donor compartments (when filled) were stirred at ~1000 rpm. The water-jacketed cells were kept at 37°C via a recirculating water bath.

Donor solution consisted of saturated DEP in buffer. An excess of DEP was added to buffer and vortexed ~24 h at room temperature. The mixture was centrifuged (3000 rpm for 30 min) and the supernatant was used as donor.

Two of the six skin disks were assigned to one of three exposure protocols, corresponding to the two cases described in the Theoretical Framework section plus an infinite dose exposure. For all three exposure protocols, 5 ml of saturated DEP were added to each of the six donor compartments at time zero.

Infinite Dose Experiments

The skin disks were exposed to donor solution for the duration of the experiment (4 h).

Transient Exposure Experiments

Case 1: Transient Exposure, Zero Concentration after Exposure. At the conclusion of the exposure period ($T_1 = 40$ min), donor solution was pipetted from the donor compartments. The donor compartments were rapidly rinsed 3–4 times with fresh buffer, and finally 5 ml of fresh buffer were placed in the well-stirred donor cells for the remainder of the experiment. The intention here was to keep the concentration at the skin surface very small, which would mimic the case of a highly volatile compound that evaporates quickly from the skin surface following the exposure period.

Case 2: Transient Exposure, Zero Flux after Exposure. At the conclusion of the exposure period (40 min, same as Case 1), donor solution was pipetted from the cells. The donor compartments were rapidly rinsed 3–4 times with fresh buffer, then the skin surfaces were gently patted with a cotton swab. Donor cells remained empty for the remainder of the experiment. Because of the low vapor pressure of DEP, flux out of the skin surface following the exposure period is expected to be minimal.

Sampling Protocol

For all experiments, 1.5 ml samples were drawn from receptor compartments at times 0, 20, 40, 60, 90, 120, 180, and 240 min and placed in 2 mL autosampler vials, then capped for subsequent analysis. Removed receptor fluid was replaced with fresh buffer. Samples of donor compartment solution were also taken and diluted 1:100 in buffer for analysis of donor concentrations. From each of the eight HGPs, the mean of the two skin punches for each of the three exposure conditions was taken at each time point.

Silicone Rubber Membrane Experiments

Experiments were repeated using SRMs. SRM discs were cut from a single sheet (Pharmelast, SF Medical, Hudson, MA; nominal thickness, 0.020 in.; measured thickness of hydrated membranes, 0.410 mm). The discs were rinsed of coating powder and soaked overnight in distilled water, then mounted on diffusion cells as before. Exposure conditions and methods were the same as for the HGP skin experiments, except that T_1 was 24 min in an attempt to maintain a similar ratio of exposure time to membrane lag time, as compared with HGP skin and determined from preliminary experiments. Also the temperature of the recirculating bath was set at 23°C instead of 37°C in order to reduce the large permeation rate through SRMs compared with HGP skin. Total experiment duration was 2 h, and sample times were 0, 12, 24, 36, 48, 72, 96, and 120 min. To minimize donor depletion, donor solution was replaced at 36 and 72 min for the infinite dose

exposures. Six SRMs for each exposure group were used.

DEP Quantification

DEP concentrations were quantified using automated solid phase microextraction (SPME) and gas chromatography (GC) as described previously.[15] Briefly, 85 μm polyacrylate SPME fibers were used (Supelco, Bellefonte, PA), and a new, conditioned fiber was used for each experiment. Extraction procedures were automated with a Combi Pal autosampler (CTC Analytics, Zwingen, Switzerland). The fiber was immersed in warmed (40°C), agitated sample for 45 min, then desorbed in the injector of a Varian CP-3800 GC (Varian, Inc., Walnut Creek, CA) with flame ionization detector. GC conditions were as described.[15] The current analyses incorporated known standards which were included at the start of each run and after every 8–12 samples. A gradual decrease in the SPME fiber response that was observed over the course of an experimental run that included over 50 samples was compensated for by linear regression of the GC response to these known standards. A calibration was performed prior to each experiment with concentrations from 0.1 to 10 μg/mL, a range that encompassed all sample concentrations except those at time zero.

From the measured concentrations, the cumulative amount of DEP penetrating each membrane was calculated, accounting for the amount of DEP removed with each sample.

DEP Saturation

The average saturation concentration of DEP in buffer was found to be 895 μg/mL. Thus ~4500 μg of well mixed DEP were available for penetration from the 5 ml donor compartments. Infinite dose conditions were approximated for HGP experiments (total accumulation <200 μg) and SRM experiments (total accumulation ~1000 μg but donor solution was changed at 36 and 72 min). Maximum receptor compartment concentrations of DEP were <20 μg/ml for HGP experiments and <60 μg/ml for SRM experiments, suggesting that sink conditions were well-approximated in the receptor compartments.

Data Analysis

Nonlinear regression was used to compare the mass accumulation data from HGP skin and SRMs with predictions of the diffusion equation for the particular exposure conditions. This analysis provides estimates for parameter values that give the best fit of the diffusion equation solutions to the experimental data.

Infinite Dose Experiments

For the exposure conditions representing infinite dose experiments, the time domain solution is well known and given by Crank:[8]

$$m(t) = k_p C_1 t - k_p C_1 \tau - \frac{12 k_p C_1 \tau}{\pi^2} \sum_{n=1}^{\infty} \frac{(-1)^n}{n^2} \exp\left(\frac{-n^2 \pi^2 t}{6\tau}\right) \quad (25)$$

There are two unknown parameters that determine the solution of this equation: permeability coefficient k_p and lag time τ. Nonlinear regressions of the mass accumulation data with Eq. (25) were performed using SigmaPlot 9.0 (Systat, Inc., San Jose, CA). The equation was truncated to seven terms in the series. Use of Eq. (25) is mathematically equivalent to calculating k_p from the slope of the steady-state DEP accumulation curve and τ as the intercept of this asymptote with the time axis. However, use of Eq. (25) is quantitatively precise and eliminates subjectivity of the analyst in these determinations.

Transient Exposure Experiments

Nonlinear regressions of the transient exposure mass accumulation data for Case 1 and Case 2 were performed using the software package Scientist 2.0 (MicroMath Scienfic Software). Regression of Case 1 data with Eq. (6), and of Case 2 data with Eq. (19) (which uses Eqs. (14, 15, 17, and 18)), yielded estimates of k_p and τ.

Statistical Analyses

Statistical analyses were performed using SigmaStat 3.11 (Systat, Inc.). Differences in the estimated quantities k_p and τ among treatment groups (infinite dose; transient exposure Case 1; transient exposure Case 2) were detected using One Way Analysis of Variance (ANOVA). If a difference ($p < 0.05$) was detected, all pairwise multiple comparisons were performed using the Holm-Sidak test. One Way ANOVA was also performed on HGP skin disc weights.

Estimates of total mass accumulation from experimental estimates of k_p and τ were made using Eq. (7) (Case 1) or Eq. (21) (Case 2) with measured values of C_1. Comparisons were made between the estimates derived from transient dose experiments with estimates based on the parameters derived from infinite dose experiments, using paired t-tests.

RESULTS

Figure 2 displays modeled flux and mass accumulation data for both Case 1 and Case 2 transient exposures. Membrane properties and input concentration are the same for all simulations, and flux and mass accumulation are shown for different exposures ranging from 0.25τ to 4τ. Case 2 results differ from Case 1 in that there is a longer relaxation time for flux following the exposure time. For a given exposure time, there is greater overall mass accumulation for Case 2 exposures compared with Case 1, but the difference diminishes as exposure time increases. These features are consequences of the different post exposure boundary conditions as discussed subsequently (Discussion).

Figure 3 compares total mass accumulations from Case 1 and Case 2 post exposure boundary conditions. Displayed is the ratio of Case 2 to Case 1 total mass accumulation; that is, the ratio of Eq. (22) to Eq. (7), as a function of exposure time relative to lag time (T_1/τ). Greater mass accumulations are predicted for Case 2 exposures compared with Case 1, as seen also in Figure 2, but for large T_1/τ, the ratio of mass accumulations approaches 1. For $T_1 > 2\tau$, for example, there is less than a twofold difference in the predicted mass accumulations from the two equations.

Modeled data from a multiple transient Case 1 exposure are displayed in Figure 4. Input concentration, flux and mass accumulation are shown for exposures of different magnitudes

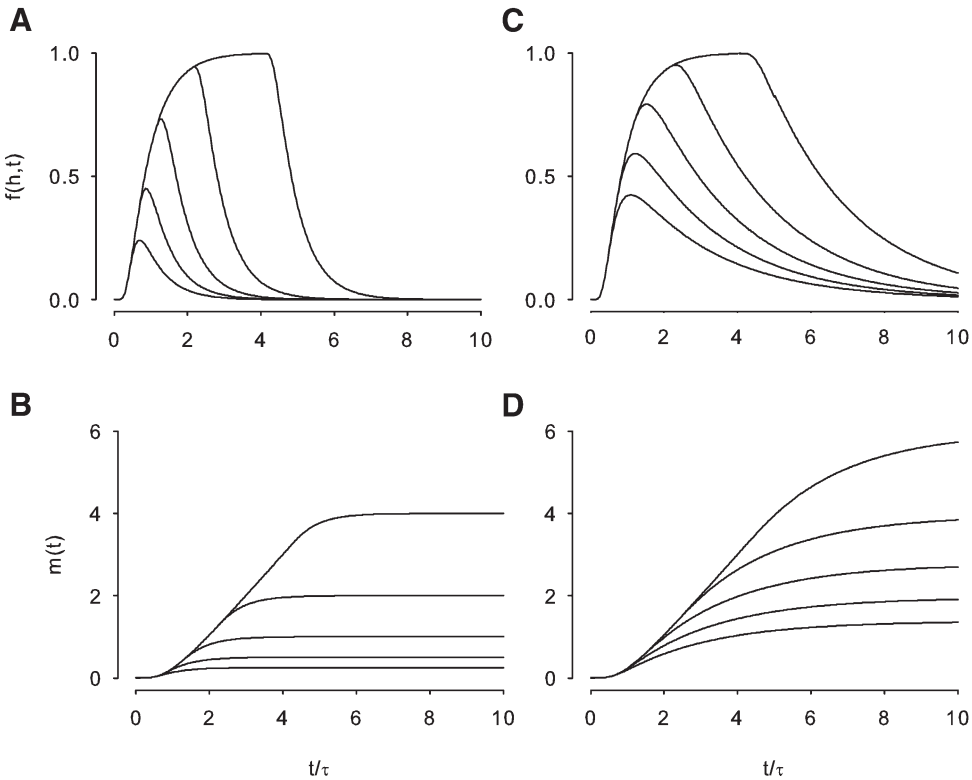

Figure 2. Transient exposure model results. Flux at lower surface ($f(h, t)$) and mass accumulation ($m(t)$) are shown for Case 1 (A and B) and Case 2 (C and D) transient exposures. Results from various exposure times are shown: 0.25τ; 0.5τ; 1τ, 2τ, and 4τ, with increasing exposure times corresponding to increasing total mass accumulation curves. Membrane properties and input concentrations are same for all simulations. All quantities are arbitrary units. Time is normalized by membrane lag time τ.

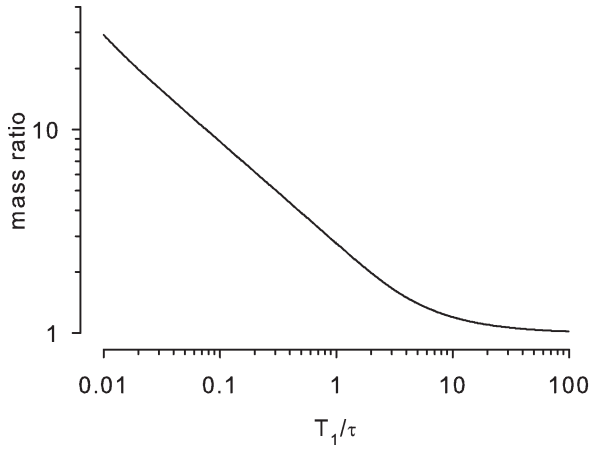

Figure 3. Ratio of total mass accumulations from zero flux (Case 2) and zero concentration (Case 1) post exposure boundary conditions. Curve displays ratio of Eq. (22) to Eq. (7), as a function of exposure time/lag time (T_1/τ).

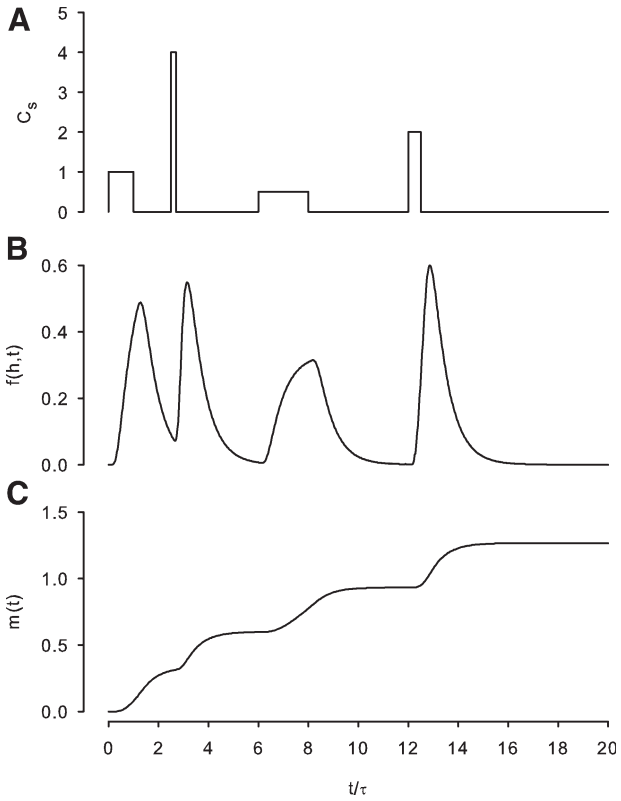

Figure 4. Multiple Case 1 transient exposure model results. Input surface concentration (C_s, A) and model results for flux at lower surface ($f(h, t)$, B) and mass accumulation ($m(t)$, C) are displayed. All quantities arbitrary units.

and durations. Note that it is not required to reach a steady-state level of flux prior to changes in the input concentration.

Turning to the experimental data, there were no detectable differences in HGP skin disc weights among the three experimental groups. Means ± SD (mg; $n = 16$ per group) were: 105 ± 24 (infinite dose); 105 ± 16 (Case 1); 106 ± 23 (Case 2). Assuming a density of 1000 mg/cm^3, these $^3/_4''$ diameter disc weights correspond to dermatomed skin thicknesses (μm) of 370 ± 84, 369 ± 55, and 374 ± 80 respectively.

Figure 5 displays DEP cumulative penetration data from the hairless guinea pig skin experiments. Panel A shows infinite dose experiments; Figure 5B shows Case 1 transient dose experiments, and Figure 5C displays Case 2 transient dose data. Experimental data are shown as means and standard deviations (SDs) from $n = 8$ HGPs. The solid lines are best-fit regressions of the data through the mean experimental values, and the estimates for k_p and τ determined from these regressions are given in the figures. The dashed lines in Figure 5B and C represent the predicted mass accumulation for these transient exposure experiments based on the values of k_p and τ determined from the infinite dose experiments.

Figure 6 displays the corresponding DEP penetration data for experiments using SRMs. These data represent experiments from $n = 6$ SRMs for each exposure condition.

Figure 7 displays the early time cumulative penetration data for the different exposure conditions from HGP (Fig. 7A) and SRM (Fig. 7B) experiments. Up until exposure time T_1 (40 min for HGP; 24 min for SRM), the membranes are exposed to the same infinite dose conditions. Therefore there should be no differences up until this time in the mass accumulations among the three exposure groups. Figure 7 shows that this is the case, and therefore the different regressions that were found for different post exposure boundary conditions were not influenced by some spurious variation among the different groups. For clarity, data points have been slightly offset on the time axis. The solid lines correspond to the infinite dose regressions.

Permeability and lag time data are given in Table 1. These data are the means and SDs calculated from all HGPs or SRMs individually. Therefore mean values may differ from the quantities given in Figures 5 and 6, which represent values that were derived from all experiments pooled. ANOVA revealed no statistically

 DOI 10.1002/jps

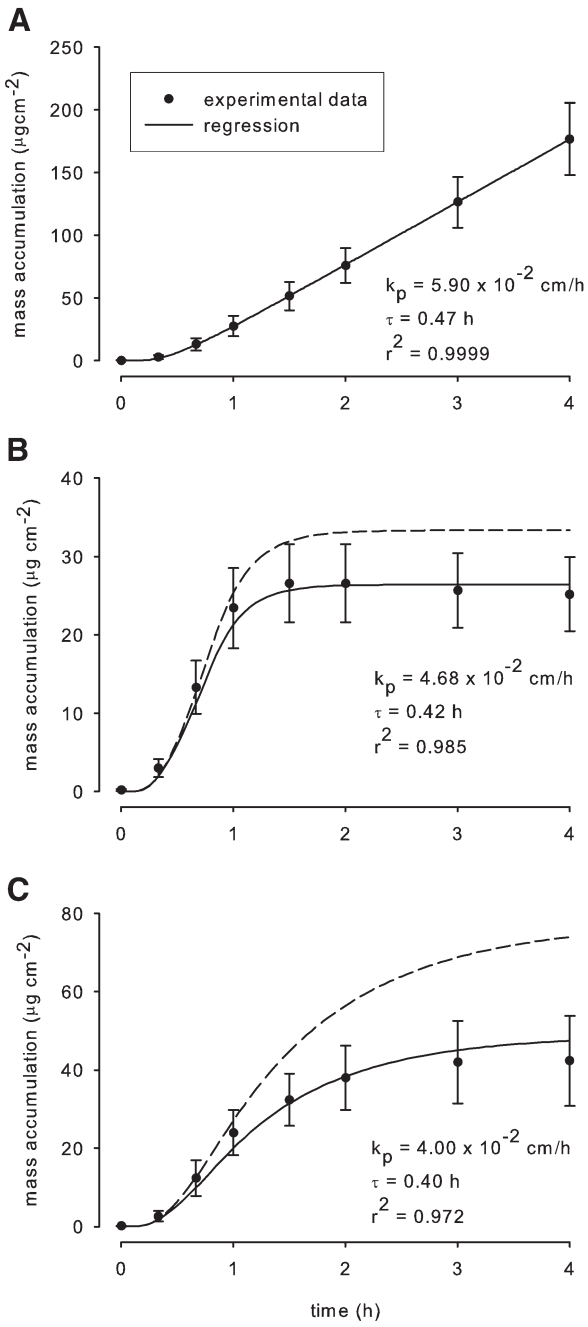

Figure 5. DEP penetration through hairless guinea pig skin. Mass accumulation through the skin from infinite dose (A) and Case 1 (B) and Case 2 (C) transient exposures (exposure time = 40 min) are displayed. Data represent means ± SD for $n = 8$ HGPs. Solid lines are best fit regression curves for the given exposure conditions as described in text, with resulting parameter values for permeability (k_p) and lag time (τ). r^2 is the coefficient of determination. Dashed lines in (B) and (C) represent predicted mass accumulations based on the values of k_p and τ determined from the infinite dose experiments.

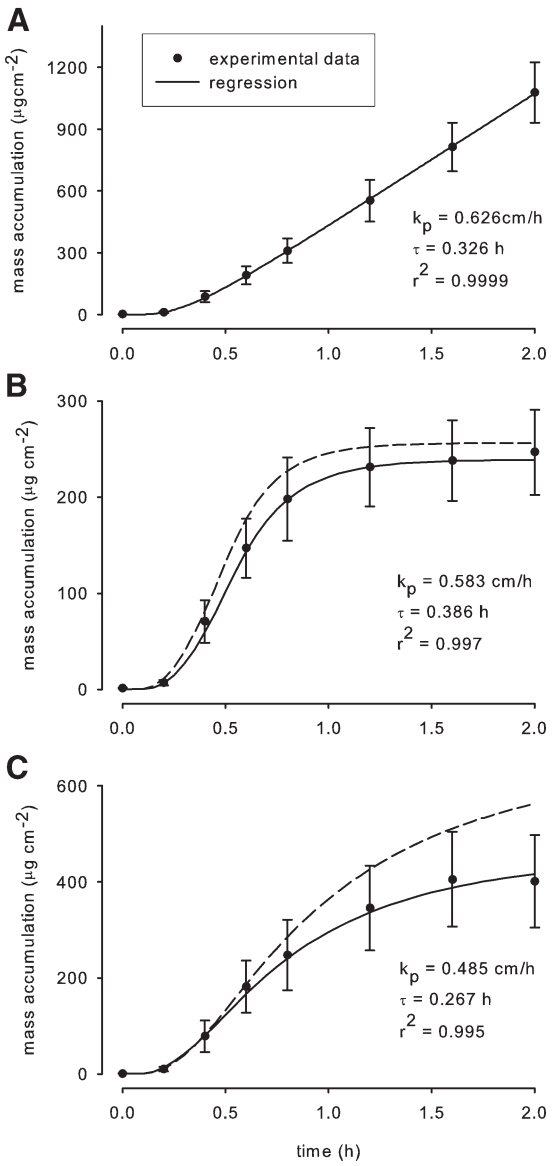

Figure 6. DEP penetration through silicone rubber membranes. Mass accumulation through the membranes from infinite dose (A) and Case 1 (B) and Case 2 (C) transient exposures (exposure time = 24 min) are displayed. Data represent means ± SD for $n = 6$ SRMs. Solid lines are best fit regression curves for the given exposure conditions as described in text, with resulting parameter values for permeability (k_p) and lag time (τ). r^2 is the coefficient of determination. Dashed lines in (B) and (C) represent predicted mass accumulations based on the values of k_p and τ determined from the infinite dose experiments.

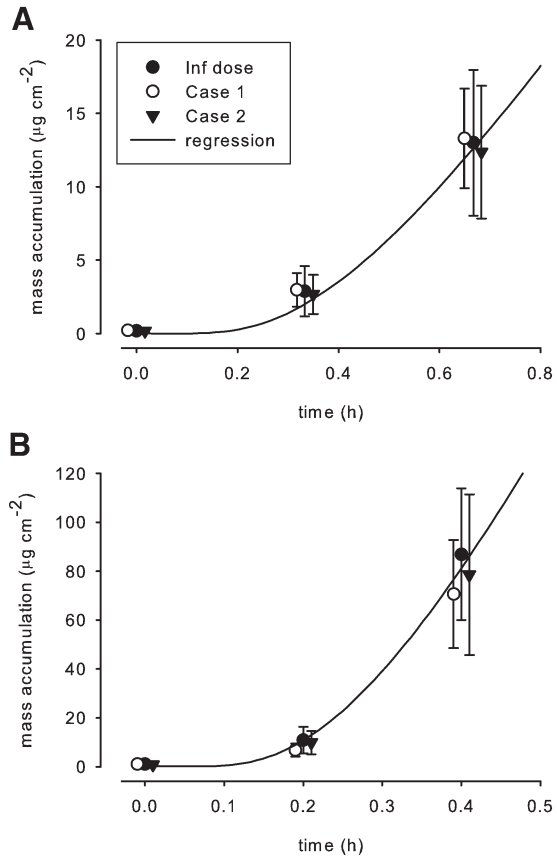

Figure 7. Early DEP penetration data from hairless guinea pig skin (A) and silicone rubber membrane (B) experiments. Means ± SD's are shown for the durations of the exposure times. The data demonstrate that no differences exist among the groups during the time in which all were subjected to the same exposures. For clarity, data points have been slightly offset on the time axis. The solid lines correspond to infinite dose regressions performed over the entire time course of exposures.

significant differences in k_p measured in SRM; in τ measured in SRM; or in τ measured in HGP skin. A difference was detected in k_p measured in HGP skin. Pairwise comparisons found a significant difference between k_p measured from infinite dose experiments compared with k_p measured from either Case 1 or Case 2 transient dose exposures, but no difference between k_p measured from Case 1 compared with Case 2 exposures.

Table 2 presents estimates of total mass accumulation from the transient exposures. These estimates were obtained from Eq. (7) (Case 1) or Eq. (21) (Case 2) using parameter values summarized in Table 1. There were significant differences between calculations based on the transient dose exposures compared with estimates based on infinite dose experimental parameters, for all cases except Case 1 studies in SRMs. In all cases, the use of infinite dose experimental parameters overestimated the total mass accumulation that was measured from the transient exposures. This holds true not only for the mean values reported here, but also for all eight individual Case 2 HGP experiments and all six Case 2 SRM experiments, as well as seven of eight Case 1 HGP but only three of six Case 1 SRM experiments.

DISCUSSION

Estimation of the disposition of chemicals applied to skin as transient exposures is a complex problem. Despite the importance of this topic in occupational, environmental, pharmaceutical, and cosmetic applications, little work has been performed in this area that can be quantified within a reasonable analytical framework. In this study, straightforward solutions to the problem have been made by adopting simplifying assumptions about the skin and physical characteristics of the applied chemical and its interaction with skin. In particular, skin is considered to be an effective homogeneous membrane; the applied chemical is assumed either to be very volatile or not at all volatile; and there is no interaction of the applied chemical with skin. With these assumptions, Laplace domain solutions to the diffusion

Table 1. Estimates of Permeability Coefficient (k_p) and Lag Time(τ) of DEP from Different Exposures

	Hairless Guinea Pig Skin ($n = 8$)		Silicone Rubber Membranes ($n = 6$)	
	k_p (cm/h)	τ (hr)	k_p (cm/h)	τ (h)
Infinite dose	0.059 ± 0.006	0.50 ± 0.17	0.628 ± 0.037	0.34 ± 0.08
Transient, Case 1	$0.047 \pm 0.009^{\dagger}$	0.40 ± 0.10	0.595 ± 0.110	0.39 ± 0.04
Transient, Case 2	$0.041 \pm 0.009^{\dagger}$	0.35 ± 0.13	0.513 ± 0.143	0.32 ± 0.06

Values are means ± standard deviations for the indicated number (n).
†Significantly different ($p < 0.05$) from infinite dose value.

Table 2. Total Mass Penetration of DEP from Transient Exposures Compared with Predicted Values Derived from Infinite Dose Experiments

	Hairless Guinea Pig Skin ($n = 8$)		Silicone Rubber Membranes ($n = 6$)	
	Transient Dose Prediction	Infinite Dose Prediction	Transient Dose Prediciton	Infinite Dose Prediction
Transient, Case 1	$26.5 \pm 4.4^{\dagger}$	33.6 ± 5.0	244 ± 51	256 ± 15
Transient, Case 2	$46.5 \pm 12.5^{\dagger}$	79.6 ± 17.6	$460 \pm 108^{\dagger}$	648 ± 80

Amounts ($\mu g/cm^2$) calculated by Eq. (7) (Case 1) or Eq. (22) truncated to five terms (Case 2), using values summarized in Table 1. Exposure times were 40 min (HGP) or 24 min (SRM).

Values are means $\pm$ standard deviations for the indicated number (n).

†Significantly different ($p < 0.05$) from prediction based on infinite dose experiments.

equation for the transient dose condition have been found. The applicability of these solutions has been explored through *in vitro* experiments in which skin or SRMs were briefly exposed to a model chemical. The use of side-by-side diffusion cells and a low volatile test compound, while controlling the conditions at the donor side of the skin during the post exposure period, allowed us to approximate both extremes of post exposure boundary conditions using one chemical, diethyl phthalate. This process in turn permits quantitative comparisons among the diffusion parameter estimates that are obtained from the different experimental conditions.

The experimental data shown here in Figures 5 and 6 demonstrate the robustness of the developed theory. In general, the experiments are well described by the solutions to the diffusion equation for the given exposure conditions. A good measure of this is the coefficient of determination, r^2, which indicates the closeness of fit between the data and the model equation (1.0 being a perfect fit). While the infinite dose experiments produced excellent r^2 (>0.999), very good correlations also resulted from the pooled transient dose experiments describe here, with $r^2 > 0.97$ for HGP skin and $r^2 > 0.99$ for SRM.

However, if the homogeneous membrane approximation is valid and experimental boundary conditions are as described, then parameter estimates for all exposure conditions should be identical. For example, permeability and lag times estimated from the infinite dose HGP experiments should be able to predict the time course of mass accumulation for either of the transient dose regimes. This is important because it would be of great benefit if transient exposures could be predicted from the more common and simpler to perform experiments using an infinite dose. In Figures 5 and 6, the dashed lines in (B) and (C) indicate the predicted mass accumulations based on the measured k_p and τ from the infinite dose experiments. The data indicate significant trends in that the parameters derived from infinite dose experiments predict greater levels of mass accumulation than those measured from the transient exposure experiments, particularly for the Case 2 studies (C). Statistical analysis verifies that the estimate of k_p from infinite dose HGP experiments is significantly greater than the estimates obtained from either transient exposure. Consequently, the use of k_p and τ derived from infinite dose studies overestimates total mass accumulation from either Case 1 or Case 2 transient exposures, as demonstrated from the data in Table 2.

By repeating the experiments with SRMs, we were able to investigate skin membrane heterogeneity as a possible explanation for the disparities between the measured transient exposure mass accumulations and the predictions from infinite dose experiments. Silicone rubber forms a simple homogeneous membrane, therefore estimates of k_p and τ from any of the three exposures should not differ. The data (Tab. 1; Fig. 6) indicate that, although there are no significant differences detected with the number of experiments performed here, there are definite trends similar to those observed with the HGP studies. The infinite dose experiments tend to over predict mass accumulation, particularly in Case 2 studies where a significant difference was detected (Tab. 2).

There are several possible explanations for these observations. One possibility relates to non homogeneous diffusion properties of skin. Watkinson et al.[16] explored depth dependent diffusion coefficients but found little effect on modeled steady-state concentration profiles. Anissimov and Roberts[17] modeled SC diffusion

and partition coefficient heterogeneity and found that it could explain reported discrepancies between penetration and desorption experiments. The split-thickness HGP skin samples used here contained both stratum corneum and viable epidermis. These layers have different permeability properties and it is likely that these differences have much larger effect than depth dependent diffusion within the stratum corneum itself. Support for some mechanism related to skin heterogeneity is given here by a comparison between HGP skin transient dose experiments with SRM transient dose experiments. The later exhibit a much smaller difference in mass accumulation from that predicted by the infinite dose experiments. These data are more in accordance with the homogeneous membrane theory than the HGP data.

Another contributing factor could be the finite time required for washing of the membranes. This time was purposely kept as brief as possible. Nevertheless, some diffusion surely occurred between the membrane (skin or SR) and the buffer during the time the membrane was in contact with the washing solution. This would lessen the amount of compound in the membrane at the end of the exposure period compared with what was assumed by the ideal boundary conditions. Because the wash time is short, a reasonable worst case estimate of the amount lost during washing can be made by assuming diffusion out of a semi-infinite membrane into a sink, as follows:[18]

$$M_{\text{wash}} = 2Ak_{\text{p}}C_1\sqrt{\frac{6t_{\text{wash}}\tau}{\pi}} \qquad (26)$$

With a liberal wash time (t_{wash}) estimate of 1 min, ~8.5 μg of DEP could have been lost during wash from the HGP skin, and ~75 μg from the SRMs. The overall result could be a significant decrease in the measured mass accumulation following the exposure period, as was observed.

Although we deliberately selected a compound (DEP) with low volatility for these studies, another factor contributing to the observed results could have been evaporation of the compound. Some evaporative flux through the membrane surface could account for the discrepancies observed for Case 2 data in both HGP and SRM experiments.

A final factor that we have considered is the possible binding of DEP to skin elements. Irreversible or slowly reversible binding of DEP to skin would lead to mass accumulation curves that exhibit features displayed in Figure 5. That is, binding of DEP would lessen the amount of DEP that desorbed from the membrane following the exposure period.

Any or all of these factors could have contributed to the observed phenomenon. Interestingly, however, the model presented here exhibits a superior ability to predict the transient exposure data from parameters derived from infinite dose experiments than the more complex multilayer model described by Krüse et al.[19] was able to predict finite dose mass accumulation from infinite dose data. Reasons for this are not known. Krüse et al. claim their finite dose model predictions are adequate when restricted to limited exposure times, and it is not clear from their description how they handle post exposure boundary conditions. We studied only one compound here while Krüse et al. presented data on five compounds exhibiting a range of lipophilicities. It remains to be seen if the present model can be validated with additional compounds and exposure times.

From the standpoint of dermal risk assessment, the main quantity of interest is the total amount of permeant that penetrates the skin in response to an exposure. It is important to keep in mind that this total includes the amount that accumulates up until the end of the chemical exposure, plus the amount that accumulates *after* the exposure period, that is, after the chemical is removed from the skin surface, from the skin depot. Eqs. (7), (12), (22), and (23) are algebraic expressions that may prove useful for exposure assessment. Eq. (7) is what one would obtain if one naively applied the steady state absorption rate (flux) to the entire exposure period, without consideration of initial transient absorption prior to establishment of steady state or absorption that continues following the exposure period. In fact, a rearrangement of Eq. (7) has been proposed as a means of estimating the exposure time required for skin absorption to reach a specified level.[20] The current analysis places Eq. (7) on firm theoretical ground and clarifies the limitation that it should only be used for highly volatile compounds, or for compounds that are continually washed away from the skin surface, or for non volatiles when exposure time is much greater than membrane lag time. For exposures from non volatiles when T_1 is not $\gg\tau$, Eq. (22) is the appropriate expression. Eq. (22) places an upper limit on the amount of chemical that penetrates the skin from transient

exposures, as it assumes that all chemical within the skin at the end of the exposure period will eventually penetrate. This upper bound could serve as a conservative estimate for risk assessment. Unfortunately, there is not much reliable lag time data in the literature that would allow broad use of this equation at this time. For moderately long exposure times, for example $T_1 \geq \tau$, Eq. (23) can be used as a simpler form of Eq. (22).

Comparison of Eq. (22) with Eq. (7) shows that predicted total mass accumulation from Case 2 transient exposures exceeds that of Case 1 exposures, all other conditions being equal (Fig. 3). This can be understood on the basis of the post exposure boundary conditions. For the two cases, the total mass accumulation is the same up until the end of exposure time (T_1). Afterward, for Case 2 all the permeant in the membrane at the end of the exposure period must penetrate the lower membrane surface ($x = h$). For Case 1, some of the permenat in the membrane at the end of the exposure period penetrates the lower surface, but some diffuses outward through the upper surface ($x = 0$) as well, depending on the local concentration gradient within the membrane. Therefore, total accumulation in Case 2 exceeds that of Case 1. Also, the time required to reach steady state after T_1 is longer for Case 2 (Fig. 2) because of the overall greater distance within the membrane that the bulk of permeant must traverse, and because diffusion time is proportional to the square of the molecules' mean displacement.

In conclusion, the model proposed here accounts for more realistic exposure scenarios than the more common theory that considers only the steady state response to an infinite dose. This theory provides a framework for estimating occupational, cosmetic and pharmaceutical dermal exposures that are transient or intermittent in nature. When used in conjunction with the related finite dose theory, a wide variety of realistic dermal exposure scenarios can be analyzed.

ACKNOWLEDGMENTS

The authors are grateful to Prof. Annette L. Bunge of the Colorado School of Mines for helpful discussions.

REFERENCES

1. Albery WJ, Hadgraft J. 1979. Percutaneous absorption: Theoretical description. J Pharm Pharmacol 31:129–139.
2. Guy RH, Hadgraft J. 1980. A theoretical description relating skin penetration to the thickness of the applied medicament. Int J Pharm 6:321–332.
3. Cooper ER, Berner B. 1985. Finite dose pharmacokinetics of skin penetration. J Pharm Sci 74:1100–1102.
4. Kubota K, Yamada T. 1990. Finite dose percutaneous drug absorption: Theory and its application to in vitro timolol permeation. J Pharm Sci 79:1015–1019.
5. Anissimov YG, Roberts MS. 2001. Diffusion modeling of percutaneous absorption kinetics: 2. finite vehicle volume and solvent deposited solids. J Pharm Sci 90:504–520.
6. Kasting GB. 2001. Kinetics of finite dose absorption through skin 1. Vanillylnonanamide. J Pharm Sci 90:202–212.
7. Kasting GB, Miller MA. 2006. Kinetics of finite dose absorption through skin 2: Volatile compounds. J Pharm Sci 95:268–280.
8. Crank J. 1975. The mathematics of diffusion. 2nd edition. Oxford: Clarendon Press. pp 49–52.
9. Carslaw HS, Jaeger JC. 1959. Conduction of heat in solids. 2nd edition. p 126.
10. Frasch HF. 2002. A random walk model of skin permeation. Risk Anal 22:265–276.
11. Frasch HF, Barbero AM. 2003. Steady-state flux and lag time in the stratum corneum lipid pathway: Results from finite element models. J Pharm Sci 92:2196–2207.
12. Nitsche JM, Wang T-F, Kasting GB. 2006. A two-phase analysis of solute partitioning into the stratum corneum. J Pharm Sci 95:649–666.
13. Hazardous Substances Data Base. DIETHYL PHTHALATE http://toxnet.nlm.nih.gov/cgi-bin/sis/search/f?./temp/~WJO4PA:1.
14. Api AM. 2001. Toxicological profile of diethyl phthalate: A vehicle for fragrance and cosmetic ingredients. Food Chem Toxicol 39:97–108.
15. Frasch HF, Barbero AM. 2005. Application of solid-phase microextraction to in vitro skin permeation experiments: Example using diethyl phthalate. Toxicol In Vitro 19:253–259.
16. Watkinson AC, Bunge AL, Hadgraft J, Naik A. 1992. Computer simulation of penetrant concentration-depth profiles in the stratum corneum. Int J Pharm 87:175–182.
17. Anissimov YG, Roberts MS. 2004. Diffusion modeling of percutaneous absorption kinetics: 3. Variable diffusion and partition coefficients, consequences for stratum corneum depth profiles and desorption kinetics. J Pharm Sci 93:470–487.

18. Crank J. 1975. The mathematics of diffusion. 2nd edition. p 32.
19. Krüse J, Golden D, Wilkinson S, Williams F, Kezic S, Corish J. 2007. Analysis, interpretation, and extrapolation of dermal permeation data using diffusion-based mathematical models. J Pharm Sci 96: 682–703.
20. Walker JD, Whittaker C, McDougal JN. 1996. Role of the TSCA interagency testing committee in meeting the U.S. government data needs: Designating chemicals for percutaneous absorption rate testing. In: Marzulli FN, Maibach HI, editors. Dermatoxicology. 5th edition. Washington DC: Taylor and Francis. pp 371–381.

 DOI 10.1002/jps